

Supplementary Information 1

Experimental data

Zn isotope analyses

With the aim of further understanding metal isotopic metabolism in the human body as well as investigating the potential to use ^{66}Zn and ^{65}Cu isotopes for age assessment studies, we tested the presence of a heavy Zn isotope accumulation through time in blood of a non-circumpolar population. To this end, we analyzed the Zn isotope composition in RBC of a sample of French people older than 55 years for which we had previously analyzed $\delta^{65}\text{Cu}$ and $\delta^{56}\text{Fe}$ ¹. This data will be compared with those obtained by our team in 2011 for individuals aged between 18 and 36². As in our 2011 study, blood samples were provided by the Etablissement Français du Sang. We also present $\delta^{66}\text{Zn}$ hepatic data because, as previously mentioned, the liver plays a central role in metal transition metabolism.

Material

The Etablissement Français du Sang in Lyon provided blood samples fully documented for sex, age, and menopausal status. Blood samples were collected in Vacurette sampling tubes (Trace Elements grade). Samples from healthy livers were initially collected for biopsies in Paul Brousse Hospital, Lyon, and donated to this study. All experiments were performed in compliance with the relevant laws of the Etablissement Français du Sang.

Methods

Reagents

Macroporous anion-exchange resin AGMP-1 100–200 mesh and AG1-X8 200-400mesh came from

Biorad Laboratories. Demineralized water was produced in a Millipore Synergy system. Concentrated technical HCl and HNO₃ provided by Merck 64271 Darmstadt, Germany, were redistilled at low temperature in Picotrace fluoropolymer stills. H₂O₂ 30% Suprapur was purchased from Merck.

Chemical separation

The metals analyzed were separated on quartz columns containing 1.6 mL macroporous anion-exchange resin following Maréchal and Albarède³. Samples were loaded onto the columns in 7 N HCl and rinsed in 10 mL 7 N HCl + H₂O₂ 0.001%. Zn was eluted using 10 mL 0.5 N HNO₃. Fractions were purified using the protocol developed by Moynier et al.⁴

Isotopic measurements

Zn isotope compositions were determined on Nu 500 HR multiple-collector inductively-coupled plasma mass spectrometer (MC-ICP-MS) using wet plasma. Free aspiration mode and a sample uptake rate of 100 mL min⁻¹ were used throughout. Gas flow instrumental mass fractionation was controlled both by dual standard-sample bracketing and the addition of an external Cu standard. The isotope reference solutions used were NIST 976 (Cu) and JMC 3-0749 L (Zn). The precision (external reproducibility, two-sigmas) on the isotope ratios was 0.05‰. Zinc concentrations were determined on an Agilent 7500 CX quadrupole ICP-MS. The run conditions are listed in Table S3.

Results

Data description

Liver and erythrocytes Zn data of French people aged over 50 years are detailed in the table S2 and in Figure 4. Average values for concentrations and $\delta^{66}\text{Zn}$ are given in table S4. Liver Zn isotope composition ranges between -1.04 and -0.37‰. The $\delta^{66}\text{Zn}$ hepatic signature is depleted compared to erythrocyte isotope composition which goes from 0.24 to 0.63‰. On average, the isotopic composition of erythrocyte individuals older than 50 years is similar to that of young individuals ($\delta^{66}\text{Zn}_{\text{old}} = 0.43 \pm 0.10$ ‰ and $\delta^{66}\text{Zn}_{\text{young}} = 0.46 \pm 0.16$ ‰). There is no sex difference observable

regardless of age group (Figure 2). There is also no significant difference between age groups (Table S5). Zinc content in blood also seems to be independent from sex, according to literature data⁵ but was lower in young male RBC than in elderly male RBC. This pattern was expected because the accumulation of Zn in male RBC increases throughout life⁶. Zinc concentrations were correlated to Cu concentrations, which corroborates earlier observations of non-dried RBC samples⁷. Concentration and isotope data were not correlated.

Statistics

Elemental Zn values do not follow a normal distribution law (Shapiro-Wilk, $p < 0.01$) in contrast to Zn stable isotope values. Therefore, we performed a non-parametric Kruskal-wallis test for the concentration data, in order to evaluate significant differences between age groups. Men aged over 50 were compared to postmenopausal women, and these two groups were then compared to data of young men and women⁷. Results are shown in table S5.

Comparisons to previous studies

First studies on Zn isotope metabolism were randomly performed on whole blood or RBC. As blood Zn is mostly contained in the RBC^{8,9}, the isotopic signature of this blood component is not statistically different from that of whole blood⁷. We therefore decided to compare isotope data obtained in whole blood or RBC. Zinc RBC values of this study were statistically different from those obtained on whole blood of Yakut (t test, $p < 1.10^{-13}$). Conversely, results do not differ from whole blood Swedish, British and Belgian data or Japanese RBC values, regardless of age group (Figure 5). They also were similar to the other French whole blood values we obtained for 5 individuals in a previous study¹⁰. Standard deviations were similar in all studies, regardless of age group.

Zn isotope composition as an indicator of menopausal state?

Although we did not test the effect of menopause on Zn isotope ratios in body tissues through box modeling, we report unpublished blood and liver data here, which brings additional evidence for the absence of relationship between menopause state and blood Zn isotope ratios (Figure S1). As is the

case for Cu and Fe isotopes, Zn liver isotope signatures are very different from those of blood (Figure 3). This pattern was previously reported for the three other mammals studied so far: sheep¹¹, mice^{12,13} and cattle¹⁴. The depletion of the hepatic $\delta^{66}\text{Zn}$ signature relative to that of blood can therefore be considered as a general rule. In previous studies, we showed that pre- and post-menopausal women exhibit very different Cu isotopic signatures in their erythrocytes, which has been attributed to a differential hepatic solicitation^{15,16} involving Fe and Cu in redox reactions⁷. Similar to Van Heghe et al. (2014)¹⁷, we did not notice any Zn isotope differences between pre- and post-menopausal French women (Figure S1). However in the Yakut population, Zn isotope differences appeared between blood of young and old women. These differences were attributed to age more than a menopausal status change¹⁰ involving a decrease of metal hepatic solicitation. Thus, it seems that menopause does not influence the Zn isotope composition of human blood.

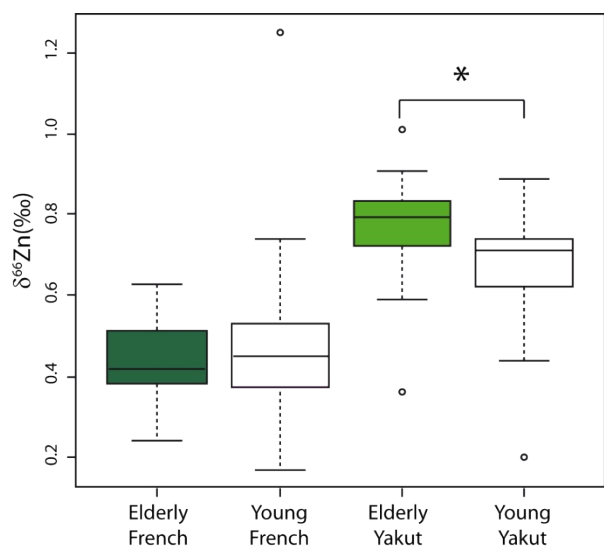


Figure S1: Zn isotope variations of Erythrocytes and liver per age group for French and Yakut populations. Whole blood data for Yakut individuals are from Jaouen et al. (2013)¹⁰. Erythrocyte data for young French individuals are from Albarede et al. (2011)⁷. The boxes represent the 25th-75th percentiles (with the median as a bold vertical line) and the whiskers show the 10th-90th percentiles. The symbol * indicates significant differences between two age group (t test, $p < 0.05$).

Zinc is not *stricto sensu* stored in the human body⁸ and, contrary to Cu, Fe hepatic sollicitation does not involve Zn in a redox reaction. The isotopic fractionation between liver and blood relies on another mechanism, probably linked to ligand bound exchanges between liver and blood circulations^{7,12,13} : zinc is associated to carbonic anhydrase in erythrocytes, whereas intracellular Zn mostly is bounded to metallothionein¹⁸ .

Supplementary Information 2

Model designing

Calibration of the Zn cycle

Body zinc composition

Mass and fluxes of the reservoirs are indicated in the table 2. Values are calibrated for a human of 70kg. The food resources are considered unlimited. The size and Zn isotope composition of urine and feces reservoirs do not influence the evolution of body $\delta^{66}\text{Zn}$ and can be chosen randomly.

Zn isotope composition of the diet

The $\delta^{66}\text{Zn}$ of terrestrial animal products are known to be between -0.7 and 0.6 ‰^{11,14,19}, and those of marine products are between -0.54 and 1.00‰¹⁹⁻²². Vegetables and seeds often show higher values^{19,23} though their isotope composition is reported as highly variable and soil dependent^{24,25}. The $\delta^{66}\text{Zn}$ value of the diet must then be between -1.0 to 1.4 ‰. In the standard model, we arbitrary fixed the value at 0.0‰. The influence of this parameter will be tested in Model B.

Zn initial isotope composition of tissues and organs

The initial value of the reservoir with a high turnover does not matter as these reservoirs will quickly reach their equilibrium values. However, for reservoirs such as muscle and bones, which have a very slow Zn turnover, we have to take into consideration this initial value while interpreting the final values. For the sake of simplicity, all the initial values have been set to 0‰.

Flux intensities:

Flux intensities derived from the fractional transfer constants (or rate constants) of kinetic models $L(i,j)$, which represent the fraction of a compartment transferred in another one per unit of time. Knowing the mass M_j of zinc in the pool j , we can establish the zinc flux between i and j (F_{i-j}) with:

$$F_{i-j}=L(i,j)*M_j$$

Partition coefficients

Values of partition coefficients are currently still unknown. We assumed that $\alpha_{a \rightarrow b}=1/\alpha_{b \rightarrow a}$ ²⁶ and that there was no isotopic fractionation during intestinal secretion ¹¹. Fractionation coefficients between each reservoir were thus estimated in such a way that steady state isotope composition of each reservoir corresponds to those published in the literature (Table 1), except for the fractionation coefficient during intestinal absorption.

For the reservoirs where $F_{A-B}=F_{B-A}$, knowing that $\alpha_{a \rightarrow b}=\frac{R_b}{R_a}$ where R is the isotope ratio of interest and b and a the two different tissues, we can simplify the relationship with the linear approximation:

$$1000*\ln(\alpha_{a \rightarrow b})=\frac{\delta^{66}Zn_b - \delta^{66}Zn_a}{x} \quad (1)$$

Where $x=2$ if $\alpha_{a \rightarrow b}=1/\alpha_{b \rightarrow a}$ and $x=1$ when $\alpha_{b \rightarrow a} = 1$

Without this factor x, the steady state values would correspond to twice that of the expected ones used for the calibration. In the case of the liver, $F_{P-L}=1/4$ of F_{L-P} and we took therefore in the equation 1, in order to estimate $\alpha_{P \rightarrow L}$, a x value of 4, and a x value of 1 for $\alpha_{L \rightarrow P}$. The rest of the hepatic input (F_{PV-L}) does not fractionate when entering the liver. The coefficient during intestinal absorption $\alpha_{I \rightarrow P}$ has been identified according the method suggested by Balter et al (2010) on sheep model ¹¹. This method consists in determining the global value for the human body (here 0.18‰). However this coefficient is lower for mice ²⁷ and its influence will therefore be tested in Model B. Expected Zn isotope composition of RBC comes from data obtained on the European and Japanese population (RBC and whole blood) ^{1,7,17,19,28,29}. Liver, serum, and bone data comes also from data obtained on human material ^{7,30, 28,29}. Currently, no muscle, skin, or kidney data have been published for humans. For muscle, we took an unpublished value of a myometrium. It implies that muscle are enriched in Zn heavy isotopes in comparison to liver, which is consistent with observations on different mammals :

mice ^{27,31}, sheep ¹¹ and bovine ¹⁴. For kidney, we considered its value is similar to the one of plasma, as recently observed in mice ²⁷. As fractionation coefficients are similar between mice and human (Table S2), we used the mice value for the coefficient between plasma and skin $\alpha_{P \rightarrow S} = 0.99965$ ²⁷

Impact of Intestinal Absorption

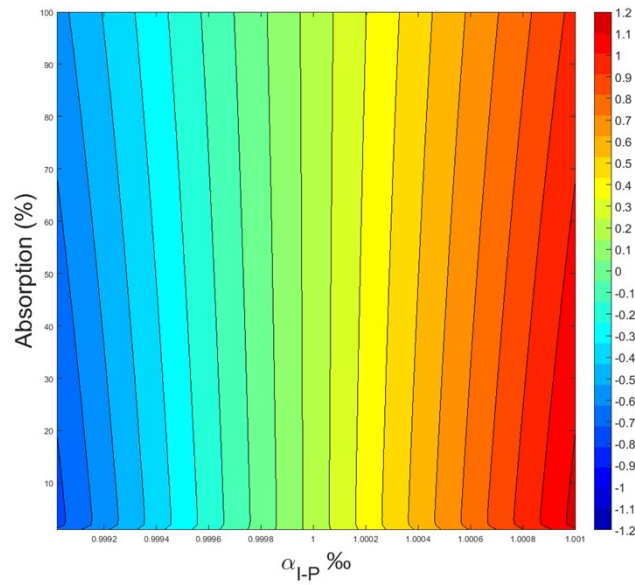


Figure S2. Respective influence of the intestinal absorption and the coefficient of isotope fractionation during intestinal absorption on the steady state Zn isotope compositions of the red blood cells.

Supplementary Information 3

Additional discussion on the implications of the model

Isotope fractionation as a function of the type of diet and metabolism

In animal feeding experiments, the dispersion of bone or blood $\delta^{66}\text{Zn}$ values is large and cannot be attributed to the sole effect of the content of phytates. Moynier et al (2013) demonstrated the effect of the genetic background on Zn isotope compositions of organs for the same species (mouse) fed with a unique diet²⁹. As mentioned above, metabolism can therefore be an additional parameter for controlling the $\alpha_{\text{L-P}}$ during intestinal absorption. Another argument for this hypothesis could be that the bone and enamel Zn isotope compositions of animals with similar diets from a single food web in Kenya had a large range of variations, but a very restricted one when species were considered separately³². The differential metabolism of circumpolar populations could then partially explain the highest $\delta^{66}\text{Zn}$ values of their blood.

Origin of the isotopic originality of Yakut's blood

The results of model B suggest a different explanation for the difference between Yakuts and other human populations and omnivores (Figure 1, 4). The $\delta^{66}\text{Zn}$ of European and Japanese diets are lower and less varied than the diet of the Yakuts. A different animal/plant

ratio in the diet is unlikely: the blood of Yakut omnivores exhibits higher $\delta^{66}\text{Zn}$ than the blood of Belgian vegetarians, whereas plant-based diets are associated to high $\delta^{66}\text{Zn}_{\text{blood}}$ values.

Rather than diet, an alternative explanation for low $\delta^{66}\text{Zn}_{\text{diet}}$ of European and Japanese populations is the anthropogenic contamination. Each year, zinc is used in many man-made items³³ and over three million metric tons are released into the environment³⁴. Zinc is incorporated into rubber to neutralize acidity, and used in agriculture as a crop nutrient. Among the populations studied for Zn isotope composition of their blood, most come from countries with a strong exploitation of zinc-ores. In fact, Japan is one of the five biggest Zn producers in the world³⁵. Respectively, Sweden and France are the first and the third Zn producers in Europe (http://sigminesfrance.brgm.fr/telechargement/substances/Pb_Zn.pdf). Belgium also produces high amounts of Zn³⁴, the isotopic consequences of which have been documented for an area of 100 km close to Gent, where the sampled population comes from³⁶. Conversely, Russia generates low levels of Zn³⁴ relative to these countries, especially in an isolated area such as Vilyuysk, the city where we conducted our former study¹⁰ (Figure S3). Zn isotopes are repeatedly suggested as potential pollution tracers^{37,38}. Sonke et al.³⁶ have outlined a model of Zn isotopic fractionation due to mining exploitation. They demonstrated that ore-grade sphalerite exhibited a homogeneous isotopic composition worldwide ($\delta^{66}\text{Zn}=+0.16\text{‰} \pm 0.20$). During Zn refining, substantial isotopic fractionation occurs with an enrichment of the vapor phase in the lighter isotopes. Particles from a Zn chimney have been documented to show values up to -0.63‰ ^{39,40}. The progressive Zn dry deposition plume generates variation in Zn isotopic compositions, which define the perimeter affected by smelting activities^{62,63}. Anthropogenic Zn contamination triggers light isotope enrichment of biological materials^{36,38,41,42}, including food products such as shellfish⁶⁶. Therefore, the low signature of European and Japanese blood may not be explained by a lower basal metabolic rate, but by a higher proportion of anthropogenic Zn in their diet relative to that of the Yakut.

Consequently, the aging drift previously reported in the Yakut population could simply be a cohort effect as market food consumption has progressively increased in this population over the last few decades^{43,44}.

It is, however, very difficult to assess if anthropogenic contamination could also explain different Cu isotopic ranges between populations. Anthropogenic Cu shows an enriched signature⁴². One should note that French blood shows significant higher values than Yakut blood, which could be linked to the incorporation of anthropogenic Cu in the French diet. However, the potential of Cu isotopes as a tracer of anthropogenic pollution has recently been challenged⁴. We now know that the isotope composition of soil impacts that of the trophic chains⁴⁵ and that diseases such as cancer and inflammation may be responsible for significant variations^{46,47}. More work is warranted to address this issue.

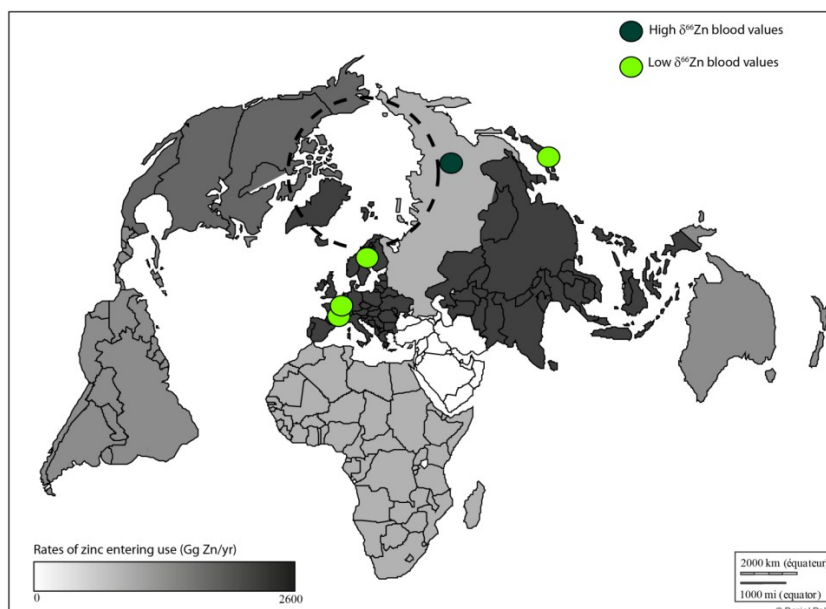


Figure S3: Zn isotope ranges and Zn rates produced each year per country. Data for rates of zinc entering use are from Graedel et al (2008). The blank map has been created by Daniel

Dalet and is available http://www.ac-aix-marseille.fr/pedagogie/jcms/c_51055/fr/cartotheque-compacte.

References

- 1 K. Jaouen and V. Balter, *Am. J. Phys. Anthropol.*, 2014, **153**, 280–285.
- 2 F. Albarède, P. Telouk, A. Lamboux, K. Jaouen and V. Balter, *Metallomics*, 2011, **3**, 926–933.
- 3 C. Maréchal and F. Albarède, *Geochim. Cosmochim. Acta*, 2002, **66**, 1499–1509.
- 4 F. Moynier, F. Albarede and G. F. Herzog, *Geochim. Cosmochim. Acta*, 2006, **70**, 6103–6117.
- 5 L. J. Hinks, B. E. Clayton and R. S. Lloyd, *J. Clin. Pathol.*, 1983, **36**, 1016–1021.
- 6 M. E. Wastney, S. Ahmed and R. I. Henkin, *Am. J. Physiol.-Regul. Integr. Comp. Physiol.*, 1992, **263**, R1162–R1168.
- 7 F. Albarède, P. Telouk, A. Lamboux, K. Jaouen and V. Balter, *Metallomics*, 2011, **3**, 926–933.
- 8 B. L. Vallee and K. H. Falchuk, *Physiol. Rev.*, 1993, **73**, 79–118.
- 9 H. Tapiero and K. D. Tew, *Biomed. Pharmacother. Bioméd. Pharmacothérapie*, 2003, **57**, 399–411.
- 10 K. Jaouen, M. Gibert, A. Lamboux, P. Telouk, F. Fourel, F. Albarède, A. N. Alekseev, E. Crubézy and V. Balter, *Metallomics*, 2013, **5**, 1016–1024.
- 11 V. Balter, A. Zazzo, A. P. Moloney, F. Moynier, O. Schmidt, F. J. Monahan and F. Albarède, *Rapid Commun. Mass Spectrom.*, 2010, **24**, 605–612.
- 12 V. Balter, A. Lamboux, A. Zazzo, P. Télouk, Y. Leverrier, A. Moloney, F. Monahan, O. Schmidt and F. Albarède, *Metallomics*.
- 13 F. Moynier, T. Fujii, A. S. Shaw and M. L. Borgne, *Metallomics*, , DOI:10.1039/C3MT00008G.
- 14 A. Stenberg, H. Andrén, D. Malinovsky, E. Engström, I. Rodushkin and D. C. Baxter, *Anal. Chem.*, 2004, **76**, 3971–3978.
- 15 K. Jaouen and V. Balter, *Am. J. Phys. Anthropol.*
- 16 K. Jaouen, L. Pouilloux, F. Albarède and V. Balter, *PLoS ONE*.
- 17 L. Van Heghe, O. Deltombe, J. Delanghe, H. Depypere and F. Vanhaecke, *J. Anal. At. Spectrom.*

- 18 R. A. DiSilvestro and R. J. Cousins, *Annu. Rev. Nutr.*, 1983, **3**, 261–288.
- 19 M. Costas-Rodríguez, L. Van Heghe and F. Vanhaecke, *Metallomics*, 2014, **6**, 139–146.
- 20 C. N. Maréchal, P. Télouk and F. Albarède, *Chem. Geol.*, 1999, **156**, 251–273.
- 21 C. N. Maréchal, E. Nicolas, C. Douchet and F. Albarède, *Geochem. Geophys. Geosystems*, 2000, **1**, 1015–15.
- 22 D. F. Araújo, G. R. Boaventura, W. Machado, J. Viers, D. Weiss, S. R. Patchineelam, I. Ruiz, A. P. C. Rodrigues, M. Babinski and E. Dantas, *Chem. Geol.*, 2017, **449**, 226–235.
- 23 F. Moynier, S. Pichat, M. L. Pons, D. Fike, V. Balter and F. Albarède, *Chem. Geol.*, 2009, **267**, 125–130.
- 24 J. Viers, P. Oliva, A. Nonell, A. Gélabert, J. E. Sonke, R. Freydier, R. Gainville and B. Dupré, *Chem. Geol.*, 2007, **239**, 124–137.
- 25 D. J. Weiss, T. F. D. Mason, F. J. Zhao, G. J. D. Kirk, B. J. Coles and M. S. A. Horstwood, *New Phytol.*, 2005, **165**, 703–710.
- 26 F. Albarède, *Introduction to geochemical modeling*, Cambridge University Press, 1996.
- 27 F. Moynier, T. Fujii, A. S. Shaw and M. L. Borgne, *Metallomics*, , DOI:10.1039/C3MT00008G.
- 28 A. Stenberg, D. Malinovsky, B. Öhlander, H. Andrén, W. Forsling, L. M. Engström, A. Wahlin, E. Engström, I. Rodushkin and D. C. Baxter, *J. Trace Elem. Med. Biol.*, 2005, **19**, 55–60.
- 29 T. Ohno, A. Shinohara, M. Chiba and T. Hirata, *Anal. Sci.*, 2005, **21**, 425–428.
- 30 K. Jaouen, V. Balter, E. Herrscher, A. Lamboux, P. Telouk and F. Albarède, *Am. J. Phys. Anthropol.*, 2012, **148**, 334–340.
- 31 V. Balter, F. Albarede, P. Telouk, A. Lamboux, K. Jaouen, A. Zazzo, A. P. Moloney, O. Schmidt and F. J. Monahan, *JAAS*.
- 32 K. Jaouen, M. Beasley, M. Schoeninger, J.-J. Hublin and M. P. Richards, *Sci. Rep.*
- 33 R. . Gordon, T. . Graedel, M. Bertram, K. Fuse, R. Lifset, H. Rechberger and S. Spatari, *Resour. Conserv. Recycl.*, 2003, **39**, 107–135.
- 34 T. E. Graedel, D. Beers, M. Bertram, K. Fuse, R. B. Gordon, A. Gritsinin, E. M. Harper, A. Kapur, R. J. Klee and R. Lifset, *J. Ind. Ecol.*, 2008, **9**, 67–90.
- 35 D. Panagapko, in *Canadian minerals yearbook*, Natural Resources Canada, Ottawa, Otario, Canada, 2009, pp. 1–56.
- 36 J. E. Sonke, Y. Sivry, J. Viers, R. Freydier, L. Dejonghe, L. André, J. K. Aggarwal, F. Fontan and B. Dupré, *Chem. Geol.*, 2008, **252**, 145–157.
- 37 C. Cloquet, J. Carignan and G. Libourel, *Environ. Sci. Technol.*, 2006, **40**, 6594–6600.
- 38 Y. Sivry, J. Riotte, J. E. Sonke, S. Audry, J. Schäfer, J. Viers, G. Blanc, R. Freydier and B.

Dupré, *Chem. Geol.*, 2008, **255**, 295–304.

39 N. Mattielli, J. C. J. Petit, K. Deboudt, P. Flament, E. Perdrix, A. Taillez, J. Rimetz-Planchon and D. Weis, *Atmos. Environ.*, 2009, **43**, 1265–1272.

40 N. Mattielli, J. Rimetz, J. Petit, E. Perdrix, K. Deboudt, P. Flament and D. Weis, *Geochim. Cosmochim. Acta*, 2006, **70**, A401.

41 S. G. John, J. Genevieve Park, Z. Zhang and E. A. Boyle, *Chem. Geol.*, 2007, **245**, 61–69.

42 M. Bigalke, S. Weyer, J. Kobza and W. Wilcke, *Geochim. Cosmochim. Acta*, 2010, **74**, 6801–6813.

43 J. J. Snodgrass, W. R. Leonard, L. A. Tarskaia, V. P. Alekseev and V. G. Krivoshapkin, *Am. J. Hum. Biol.*, 2005, **17**, 155–172.

44 T. J. Cepon, J. J. Snodgrass, W. R. Leonard, L. A. Tarskaia, T. M. Klimova, V. I. Fedorova, M. E. Baltakhinova and V. G. Krivoshapkin, *Am. J. Hum. Biol.*, 2011, **23**, 703–709.

45 K. Jaouen, M.-L. Pons and V. Balter, *Earth Planet. Sci. Lett.*, 2013, **374**, 164–172.

46 P. Telouk, A. Lamboux, V. Balter and F. Albarede, *1st Workshop Biomed. Appl. Geochem.*

47 V. Balter, F. Albarede, A. Da Costa, P. Telouk, A. Lamboux, K. Jaouen, N. Vincent, A. Brechot and P. Hainaut, *1st Workshop Biomed. Appl. Geochem.*, 2013.

Supplementary Tables

Id	Sex	Age	AM	DA-AM	GS	$\delta^{66}\text{Zn}(\text{‰})$	[Zn]ppm
3	F	55	53	2	O	0.36	29.3
4	F	56	49	7	O	0.45	34.8
11	F	63	56	7	NA	0.39	28.8
12	F	58	40	18	A1	0.38	34.7
13	F	55	51	4	O	0.61	38.2
28	F	60	55	5	A1	0.31	38.3
29	F	62	50	12	O	0.45	29.7
30	F	65	52	13	O	0.52	45.8
31	F	61	53	8	A1	0.28	32.6
32	F	60	50	10	B	0.26	31.0
33	F	59	54	5	A	0.63	37.1
34	F	62	52	10	O	0.41	31.2
35	F	66	52	14	O		43.0
36	F	60	55	5	A1	0.39	35.5
37	F	62	48	14	B	0.38	40.6
38	F	64	53	11	A	0.57	36.3
39	F	63	51	12	O	0.39	28.5
40	F	64	55	9	B	0.56	28.3
41	F	63	55	8	O	0.48	28.5
1	H	60			A1	0.40	71.1
2	H	62			A1	0.44	32.9
5	H	64			A1	0.34	31.8
6	H	65			O	0.42	34.1
7	H	61			A1	0.59	37.0
8	H	64			A1	0.51	27.7
9	H	62			A2	0.50	66.4
10	H	61			A2	0.34	31.2
14	H	65			O	0.56	33.6
15	H	65			A1	0.44	25.4
16	H	62			A	0.38	29.7
17	H	60			A2	0.56	25.3
18	H	63			O	0.24	37.,1
19	H	64			O	0.44	29.0
20	H	63			O	0.36	25.1

Table S1. Biological, elemental and isotopic data for blood of women and men Older than 50 y.o.

Id: sample identification number. AM: age at menopause Δ A-AM: number of years since the menopause BT: blood type

	mouse	minipig	human
α_{P-RBC}	1.00008	1.00005	1.00012
α_{P-M}	0.99994	NA	0.99993
α_{P-B}	1.00027	NA	1.00030
α_{P-L}	0.99965	0.99946	0.99939

Table S2. Comparison of fractionation coefficient between mouse, minipig and human.

See text for the determination of human coefficients. Mouse coefficients are based on the study of Moynier et al. 2013, minipig coefficients are from Mahan et al. 2018

Instrument	Agilent 7500 cx	Nu500 HR	Nu1700
RF power	1500 W	1350 W	1350 W
External flow	15 L ⁻¹	14L ⁻¹	14L ⁻¹
Nebuliser gas flow rate	1,1 L.min ⁻¹	1 L.min ⁻¹	1 L.min ⁻¹
Integration time	0,1s	10s per cycle	10s per cycle
Total integration time	120s	20x2 s	20x2 s
Collision/reaction gas	He	N/A	N/A
Flow rate	6 mL.min ⁻¹	N/A	N/A
Nebuliser	GE AR351FM04	GE AR351FM01	GE AR351FM02
DSN neb pressure	N/A	N/A	31 psi
Sample cone	Ni	Ni	Ni
Skimmer cone	Ni	Ni	Ni

Table S3. Summary of analytical conditions

	Mean	SD	
<i>Isotopic data</i>	$\delta^{66}\text{Zn}(\text{‰})$		
Men > 50 y.o. (OM)	0.4346	0.1	15
Postmenopausal women (OW)	0.4344	0.11	18
Liver	-1,05	0,43	9
<i>Concentrations (dried RBC)</i>	[Zn]ppm		
Premenopausal women (YW)	32.32	12.8	20
Men < 40 y.o. (YM)	28.99	8.58	20
Postmenopausal women (OW)	34.3	5.25	19
Men > 50 y.o. (OM)	35.81	13.94	15

Table S4. Average isotope compositions in delta units (permil or ‰) and 95% range (2SD) for the isotope compositions and concentrations of Zn, Cu, and Fe in the liver and erythrocytes.

Typical analytical uncertainties are 0.05 ‰.

<i>Isotopic data</i>	$\delta^{66}\text{Zn}$	
T Test results		
	t value	p
OM-OW	0,43	0,67
OM-YM ¹	-1,18	0,26
OM-YW ¹	0,41	0,69
OW-YW ¹	0,2	0,85
OW-YM ¹	-1,06	0,3
<i>Concentrations</i> [Zn]		
Kruskal Wallis results		
	χ^2	p
OM-OW	0.85	0.36
OM-YM	4.00	0.04
OM-YW	0.81	0.37
OW-YW	1.81	0.18
OW-YM	7.12	0.008*
YM-YW	0.49	0.48

Table S5. T and χ^2 results for Student and Kruskal-Wallis test performed for Cu, Fe and Zn isotope compositions and concentrations between pairs of age and sex groups.

For two populations (k-1) and a level of significance of 5% (± 0.05), χ^2 equals 3.84. For significant results, * is when $p < 0.05$.; ** is when $p < 0.005$ OM: Old men, OW: Old women; YM: Young men, YW: Young women. ¹. Young values were previously published in Albarede et al, 2011.